

## Hanle Effect in $2^1P$ Helium\*<sup>†</sup>

E. S. Fry<sup>‡</sup> and W. L. Williams

*Harrison M. Randall Laboratory of Physics, The University of Michigan, Ann Arbor, Michigan 48104*

(Received 17 January 1969)

The oscillator strength for the resonance ( $1^1S-2^1P$ ) transition in atomic helium has been determined from a measurement of the lifetime of the  $2^1P$  state. This lifetime was obtained using a modified zero-field level crossing (Hanle) method. The scattering sample was a thermal velocity beam of  $2^1S$  metastable atoms. Resonant  $2-\mu$  ( $2^1S-2^1P$ ) radiation is absorbed by the  $2^1S$  atoms, which are excited to the  $2^1P$  state. This state then primarily decays to the ground  $1^1S$  state with the emission of resonance (584 Å) radiation. The lifetime of the  $2^1P$  state was determined from measurements of the magnetic-field dependence of the angular distribution of the 584 Å intensity. This new technique eliminates the problem of constructing a vacuum ultraviolet resonance lamp. The measured lifetime  $\tau$  ( $2^1P$ ) is  $(5.63 \pm 0.22) \times 10^{-10}$  sec. The resulting absorption oscillator strength for the resonance transition is  $0.273 \pm 0.011$ . This oscillator strength agrees with the theoretical value.

### I. INTRODUCTION

An important test of approximate two-electron wave functions is provided by an experimental check of the predicted oscillator strengths or  $f$  values. Those  $f$  values predicted for transitions between the ground state ( $1^1S$ ) and the  $n^1P$  states of helium are extremely sensitive to the choice of wave functions. This sensitivity is demonstrated by the wide variations in the results of early calculations.<sup>1</sup> Recently, two-electron wave functions based on high-order approximations have been obtained.<sup>2</sup> Energy eigenvalues obtained from these wave functions agree with experimental values having errors of at most several parts per million. The  $f$  values determined with these wave functions exhibited excellent internal consistency in that the results obtained from dipole length, velocity, and acceleration matrix elements agreed within 0.02%.<sup>3</sup> The results of several other authors are comparable.<sup>4</sup>

The sensitivity of the calculated  $f$  value to the choice of the approximate wave function is especially strong for the resonance ( $1^1S-2^1P$ ) transition in helium. Kuhn and Vaughan<sup>5</sup> reported an experimental  $f$  value for this transition from an interferometric profile analysis of spectral lines terminating in the  $2^1P$  state. They obtained a value some 30% larger than the Schiff and Pekeris theoretical value. This discrepancy was rather surprising considering the apparent accuracy of the wave functions used to obtain the calculated result. Over the next several years the experimental data were confirmed, but were analyzed with an inclusion of resonance broadening effects. Vaughan<sup>6</sup> has shown that if the Schiff and Pekeris  $f$  value is used, then the experimental data are in agreement with resonance broadening theory. Korolyov and Odintsov<sup>7</sup> also used interferometric

techniques to study light produced by electron bombardment of an atomic beam. Under the conditions most favorable for determining the line width they obtained an  $f$  value with  $\approx 5\%$  error limits. However, it disagrees with the theoretical value by  $\approx 6\%$ .

In the present experiment the  $f$  value for the resonance transition in  $^4\text{He}$  is determined from a measurement of the lifetime of the  $2^1P$  state. This lifetime was measured by utilizing a zero-field optical level-crossing or Hanle-effect technique.<sup>8,9</sup> The Hanle method offers distinct advantages in that Doppler broadening effects are generally negligible and the measurements do not require a knowledge of the density of sample atoms in the low density limit. The inherent disadvantage is that it requires an intense source of the resonance radiation which is not strongly self-reversed. Normally this would be a serious problem for the present experiment since the strong radiative transition from the  $2^1P$  state is in the vacuum ultraviolet (584 Å). However this problem was eliminated by using a modified Hanle method described previously.<sup>10</sup> In this method resonant  $2^1P-2^1S$ ,  $2-\mu$  radiation is incident on a sample of  $2^1S$  metastable helium atoms. The emitted  $2^1P-1^1S$ , 584 Å radiation is observed as a function of magnetic field. The present results indicate that the construction of an intense source of  $2-\mu$  resonance radiation which is not strongly self-reversed is not difficult.

### II. THEORY

Level-crossing phenomena can be described in terms of a quantum-mechanical theory of interference effects due to Breit.<sup>11</sup> The Breit formula has been discussed by several authors.<sup>12</sup> It gives the rate  $R(\hat{f}, \hat{g})$  at which resonance radiation of

polarization  $\hat{f}$  is absorbed and radiation of polarization  $\hat{g}$  is re-emitted by a sample of atoms (see Fig. 1). Specifically we have

$$R(\hat{f}, \hat{g}) \propto \sum_{\substack{\mu, \mu' \\ m, m'}} \frac{f_{\mu m} f_{m \mu'} g_{\mu' m'} g_{m' \mu}}{1 + i\tau(E_{\mu} - E_{\mu'})/\hbar}, \quad (1)$$

where  $\mu$  and  $\mu'$  refer to excited state magnetic sublevels;  $m$  and  $m'$  refer to magnetic sublevels of the ground state;  $f_{\mu m} = \langle \mu | \hat{f} \cdot \vec{r} | m \rangle$ , etc., are dipole matrix elements;  $E_{\mu}$  is the energy of the  $\mu$ th excited sublevel, etc.; and  $\tau$  is the mean lifetime of the excited state. There are resonant effects when  $E_{\mu} = E_{\mu'}$ , that is when the energy levels cross. When they cross at zero magnetic field the phenomenon is called the Hanle effect. Generally, the initial as well as the final state is the ground state. However, for the case in which the initial and final states are different, Breit<sup>11</sup> has pointed out that (1) is still valid provided  $m$  is restricted to magnetic sublevels of the initial state and  $m'$  to sublevels of the final state. This generalization is important to the present experiment.

Figure 2 shows the spherical coordinate system used to evaluate  $R$ . Here the magnetic field  $H$  is along the  $z$  axis;  $\theta, \varphi$  are, respectively, the polar and azimuthal angles of the incident light direction; and  $\theta', \varphi'$  are corresponding angles for the observed light direction. Several authors<sup>9, 13</sup>

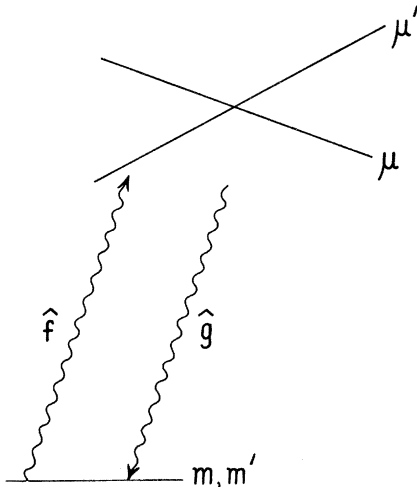


FIG. 1. Energy-level diagram for the Breit formula.

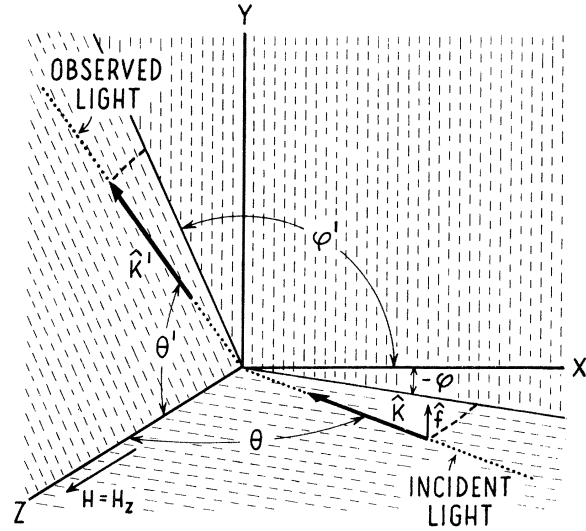


FIG. 2. Coordinate system used to evaluate the Breit formula.

have outlined the calculation of the required matrix elements. For a Hanle effect level crossing, the scattering rate in a  $J=0 \rightarrow J=1 \rightarrow J=0$  transition is given by

$$R \propto \left[ (2 - \sin^2 \theta') + \frac{\sin^2 \theta' \cos 2(\varphi' - \varphi)}{1 + x^2} + \frac{x \sin^2 \theta' \sin 2(\varphi' - \varphi)}{1 + x^2} \right], \quad (2)$$

$$x = 2g_J \mu_0 H \tau / \hbar,$$

where  $\tau$  and  $g_J$  are the mean lifetime and  $g$  value of the excited state, respectively. In Eq. (2) it is assumed that the incident light has polarization vector  $\hat{f}$  parallel to the  $y$  axis (perpendicular to the magnetic field) and the observed light is detected without regard to polarization. The field dependence is produced by interference between the  $m = \pm 1$  substates of the  $J=1$  state. Note also that this result is independent of the angle  $\theta$  of the incident light.

The geometry of the present experiment requires the average of Eq. (2) over symmetric solid angle contributions centered about a  $90^\circ-90^\circ-90^\circ$  geometry (mutually perpendicular incident light direction, observation direction, and magnetic field). We evaluate

$$\bar{R} = \int R d\Omega / \int d\Omega, \quad (3)$$

where  $d\Omega = \sin \theta \sin \theta' d\theta d\theta' d\varphi d\varphi'$  and the limits of integration are:

$$\varphi: -\alpha, +\alpha; \quad \varphi': \frac{1}{2}\pi - \beta, \frac{1}{2}\pi + \beta;$$

$$\theta: \frac{1}{2}\pi - \gamma, \frac{1}{2}\pi + \gamma; \quad \theta': \frac{1}{2}\pi - \delta, \frac{1}{2}\pi + \delta.$$

Here  $\alpha, \beta, \gamma$ , and  $\delta$  are small angles defining the extent of departure from exact  $90^\circ-90^\circ-90^\circ$  geometry. The result is

$$\bar{R} \propto \frac{2\alpha}{\sin 2\alpha} \frac{2\beta}{\sin 2\beta} \frac{3 + \sin^2 \delta}{3 - \sin^2 \delta} \frac{1}{1 + x^2}. \quad (4)$$

In the limit  $(\alpha, \beta, \gamma, \delta) \rightarrow 0$  or perfect  $90^\circ-90^\circ-90^\circ$  geometry, Eq. (4) reduces to the usual inverted Lorentzian result

$$\bar{R} \propto \left(1 - \frac{1}{1 + x^2}\right). \quad (5)$$

Recalling that the above results are obtained for polarized incident light, it is seen that Eq. (5) does give the expected result,  $\bar{R} = 0$ , when  $H = 0$  ( $x = 0$ ). However, it is also seen that the more general Eq. (4) does not necessarily yield  $\bar{R} = 0$  when  $H = 0$ . The important point here is that inclusion of the symmetric solid angle effects adds a field independent background to the inverted Lorentzian of Eq. (5). In general for unpolarized incident light, these effects reduce the ratio of field dependent to field independent signal from that ratio obtained for perfect geometry.

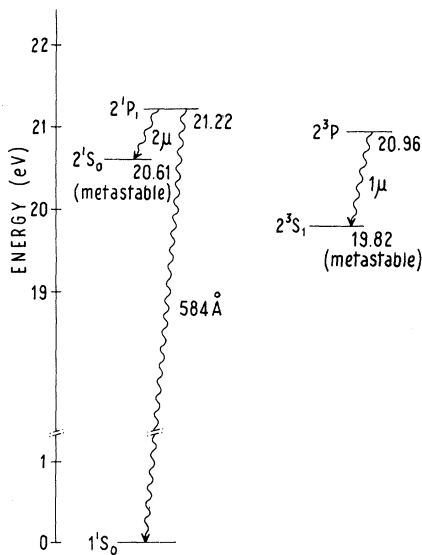


FIG. 3. Low-lying levels of helium with the allowed electric-dipole transitions indicated.

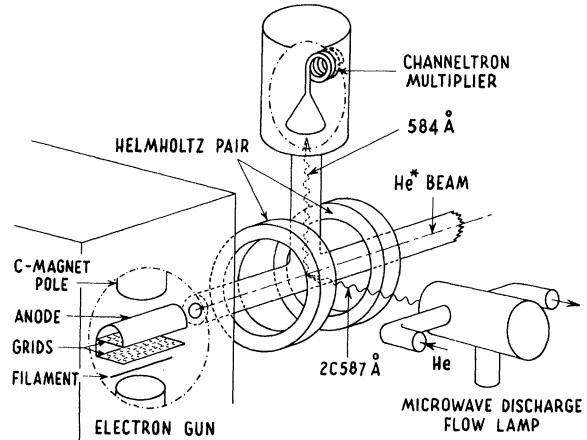


FIG. 4. Experimental arrangement for the modified Hanle effect experiment.

Setting  $x = 1$ , the relationship between the excited state lifetime and the half-width at half-maximum,  $H_{1/2}$ , of the inverted Lorentzian line is obtained,

$$\tau = \hbar / 2g_J \mu_0 H_{1/2}. \quad (6)$$

### III. EXPERIMENT

#### A. Method

Figure 3 shows an energy-level diagram of the low-lying states of  $^4\text{He}$  together with the allowed electric dipole transitions. To determine the  $2^1P$  lifetime, the usual Hanle experiment would involve scattering  $584 \text{ \AA}$  radiation from a sample of ground-state helium atoms. Unfortunately, this radiation is in the vacuum ultraviolet region of the spectrum where construction of a suitable light source is a difficult problem.

A second approach would be to treat the  $2^1S$  metastable state as a "ground state" and scatter  $2\text{-}\mu$  radiation, a wavelength for which optical instrumentation is readily available. This is analogous to the work of Colegrove, Franken, Lewis, and Sands<sup>14</sup> in which  $1\text{-}\mu$  radiation is scattered from  $2^3S$  metastable atoms. However, the transition probability for decay of the  $2^1P$  excited state to the  $1^1S$  ground state by electric-dipole radiation is more than 1000 times greater than the transition probability for decay to the  $2^1S$  metastable state. Therefore the intensity of scattered  $2\text{-}\mu$  radiation would be quite small.

These problems were avoided by performing a modified Hanle type level-crossing experiment in which the incident and scattered radiations are of different wavelengths.<sup>10</sup> Specifically, resonant

$2^1P-2^1S$ ,  $2\text{-}\mu$  radiation was used to excite helium atoms from the  $2^1S$  metastable state to the  $m = \pm 1$  substates of the short-lived  $2^1P$  state. The intensity of the  $584 \text{ \AA}$  radiation emitted during the decay of this state was then measured as a function of magnetic field.  $H_{1/2}$  and, hence,  $\tau(2^1P)$  were determined from the resulting inverted Lorentzian line shapes.

### B. Apparatus

A diagram of the experimental apparatus is shown in Fig. 4. Metastable helium atoms were produced in the electron-gun region by electron bombardment and then collimated into a beam. Resonant  $2^1P-2^1S$ ,  $2\text{-}\mu$  light from a helium discharge lamp illuminated the beam in the central region of the Helmholtz pair. The  $584 \text{ \AA}$  radiation was detected at  $90^\circ$  to the direction of this incident radiation. The Helmholtz pair provided a magnetic field parallel to the metastable beam and perpendicular to the directions of both the incident ( $2\text{-}\mu$ ) and scattered ( $584 \text{ \AA}$ ) radiations.

The electron gun is a simple diode in which the filament serves as cathode. The filament is a 2.5-cm-long, 0.2-mm in diameter thoriated tungsten wire. It was heated by passing a dc current of 4.5 A through it. The anode is a semi-cylindrical piece of 0.1-mm thick stainless steel to which two tungsten grids are attached. Electrons emitted by the filament are accelerated toward the anode by the first of these grids; the second, together with the anode, forms an electric field free region through which the electrons pass. This assembly is placed between the poles of a permanent magnet which has a field of  $\approx 300 \text{ G}$  and serves to collimate the electrons between the filament and anode. Typically, the anode voltage was +40 V with respect to the filament, and the corresponding emission current was 2 mA. The electron gun stability was improved by heating the anode to a dull red glow before each data session. This was accomplished by passing an ac current of 60 A through the anode.

The electron-gun assembly was enclosed in a box containing helium gas whose pressure was varied between  $5 \times 10^{-4}$  and  $3 \times 10^{-3}$  Torr. This box was located inside the vacuum system. The base pressure throughout the vacuum system was  $1 \times 10^{-7}$  Torr. When helium was let into the electron-gun box this pressure would rise to between  $3 \times 10^{-6}$  and  $2 \times 10^{-5}$  Torr. Opposite the electric field free region between the upper grid and the anode, there was a 5-mm in diam hole in the box through which helium atoms in various states could diffuse. These atoms were collimated into a beam which passed along the axis of the Helmholtz pair. It is reasonable to assume the beam contained only ground state ( $1^1S$ ) and metastable ( $2^1S$  and  $2^3S$ ) helium atoms, since at thermal velocities

( $\approx 10^5 \text{ cm/sec}$ ), an atom excited to an optically decaying state traveled a very short distance ( $\approx 10^{-2} \text{ cm}$ ) before decaying with a typical lifetime ( $\approx 10^{-7} \text{ sec}$ ). The distance between the collimating hole in the electron-gun box and the center of the scattering region was 10 cm.

The scattering region was a  $\frac{3}{4}$ -in. in diam Pyrex tube coaxial with the metastable beam. At a right angle to this tube and halfway between the Helmholtz coils a second Pyrex tube led to the detector chamber. By means of two adjustment screws the scattering region could be rotated, thereby moving the detector and altering the angle ( $\varphi' - \varphi$ ) between the detector and lamp.

A Bendix Channeltron electron multiplier was used for detection of the  $584 \text{ \AA}$  radiation. When 2500 V is applied across this device, it has a gain of  $\approx 10^7$  with noise of 0.1 counts/sec. It has a window from 2 to  $1400 \text{ \AA}$  with a quantum efficiency of  $\approx 25\%$  at  $584 \text{ \AA}$ .<sup>15</sup> The detecting surface is the inside of a cone which is 1 cm in diameter at the open end. This open end was 15 cm from the metastable beam. However, the effective solid angle was somewhat increased due to reflection of  $584 \text{ \AA}$  radiation from the walls of the interconnecting  $\frac{1}{2}$ -in. Pyrex tube.

Resonant  $2\text{-}\mu$  light was obtained from a helium discharge lamp which was in a microwave cavity powered by a Raytheon Microtherm diathermy machine. Helium at a pressure of  $\approx 1$  Torr flowed through a 5-mm diam quartz tube placed in cavity No. 5 of those described by Fehsenfeld, Evenson, and Broda.<sup>16</sup>

The  $2\text{-}\mu$  radiation produced was directed towards the metastable beam by means of a hollow, polished aluminum light pipe. Since this light pipe was of a divergent type, it not only increased the intensity of  $2\text{-}\mu$  light which is incident on the beam, but also decreased the angle of divergence of the reflected light. Figure 5 shows two cross sections of the light pipe. These illustrate, re-

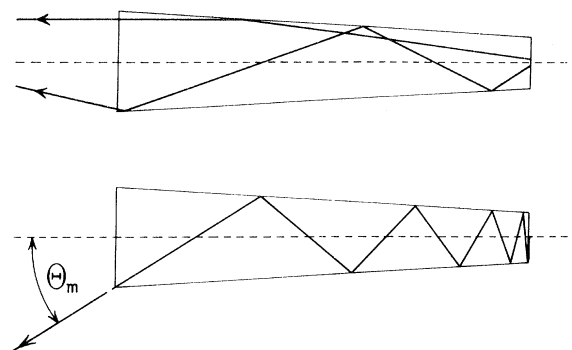


FIG. 5. Light pipe cross sections showing the path of typical light rays.  $\Theta_m$  is the maximum angle at which a light ray can exit.

spectively, the path of typical light rays, and the path of a light ray which exits at the maximum possible angle,  $\Theta_m$ , with respect to the light pipe axis.<sup>17</sup> For transmitted radiation with  $\Theta \approx \Theta_m$  the intensity is reduced since it must undergo several reflections with  $\approx 10\%$  loss in intensity at each reflection. The light pipe was 4 cm long. It had an entrance width of 0.5 cm, an exit width of 1 cm, and  $\Theta_m$  was  $33^\circ$ . The lamp was placed at the entrance to the light pipe so that light from nearly a  $2\pi$  solid angle was collected. A Polaroid HR infrared polarizer between the large end of the light pipe and the beam polarized the incident light perpendicular to the Helmholtz field.

The magnetic field was monitored by measuring the voltage across a  $0.1\text{-}\Omega$  manganin resistor which was in series with the Helmholtz coils. The field calibration was made by measuring the field with a Rawson rotating coil gaussmeter whose claimed 0.1% accuracy was verified by comparison with a low-field proton resonance probe. The axial magnetic field variation over the scattering region was 0.5%. The field from the electron-gun magnet together with the earth's magnetic field contributed 1.5 G perpendicular to the axis of the coil.

#### IV. RESULTS

##### A. Preliminary Measurements

Preliminary experiments provided an unambiguous verification that the process observed is absorption of  $2\text{-}\mu$  radiation followed by emission of  $584\text{ \AA}$  radiation. A filter which transmitted a  $0.05\text{-}\mu$  band centered at  $2.059\text{ }\mu$  was inserted between the lamp and the beam. The Hanle signal was still observed, although reduced in amplitude. When the above filter was replaced by one that had an absorption band at  $2\text{ }\mu$ , the Hanle signal was absent. Finally, when the discharge lamp was run with  $^3\text{He}$ , no Hanle signal was observed. This last result is expected since the wavelength of the  $2\text{-}\mu$  line in  $^3\text{He}$  is shorter than that in  $^4\text{He}$  by  $\approx 0.9\text{ \AA}$ ,<sup>18</sup> or  $\approx 25$  times the natural  $2\text{-}\mu$  absorption breadth.

The  $2^1S$  metastable flux and the  $584\text{ \AA}$  flux in the atomic beam direction were measured with a second Channeltron on the beam axis at a point 25 cm from the electron-gun box. Time-of-flight (TOF) techniques<sup>19</sup> were used to distinguish the radiation from the metastable atoms. The  $2^1S$  quenching technique<sup>20</sup> was used to determine the  $2^1S$  beam intensity. At a helium pressure of  $6 \times 10^{-6}$  Torr in the vacuum system the  $584\text{ \AA}$  flux was  $\approx 1.5 \times 10^{-5}$  ergs/cm<sup>2</sup> sec. and the  $2^1S$  metastable flux was  $\approx 1.8 \times 10^5$  atoms/cm<sup>2</sup> sec. These values are corrected for the TOF duty cycle and the Channeltron detection area but are not corrected for the

Channeltron detection efficiency.

##### B. Background Effects

A typical set of  $584\text{ \AA}$  counting rates is presented in Fig. 6. The data for negative and positive fields are the counting rates for opposite directions of the field. This set of data was taken at a helium pressure of  $6 \times 10^{-6}$  Torr. The background count rate that arises when there is a metastable beam in the machine and the  $2\text{-}\mu$  lamp is off is produced mainly by the scattering of  $584\text{ \AA}$  radiation originating in the electron-gun region. This count rate can be estimated as follows. Using the measured value of the  $584\text{ \AA}$  flux the intensity of the  $584\text{ \AA}$  radiation scattered in the  $1\text{-cm-long}$ ,  $\frac{3}{4}\text{-in. diam}$  scattering region can be calculated by correcting for the solid angle and the absorption between the electron gun and the beam axis Channeltron.<sup>21</sup> The result is  $1.2 \times 10^{-5}$  ergs/sec scattered into  $4\pi$  solid angle. The Channeltron used to detect the  $584\text{ \AA}$  radiation scattered at  $90^\circ$  to the beam axis has a  $1\text{-cm diam}$  detection area and was 15 cm from the beam. Correcting for this solid angle factor together with the absorption<sup>21</sup> between the beam and the detector the calculated background count rate is 60 counts/sec in agreement with the observed value of 57 counts/sec. This calculation does not include the effect

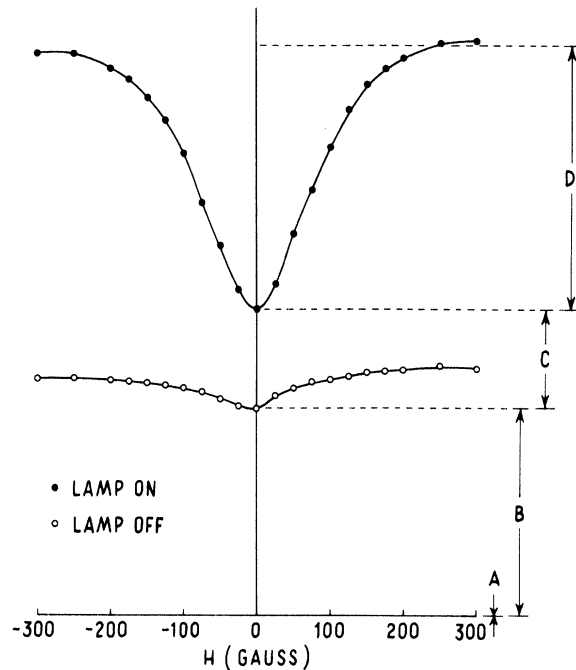


FIG. 6. Typical  $584\text{ \AA}$  counting rates: *A* – dark count rate (no metastable beam) – 0.1 counts/sec.; *B* – background count rate (with metastable beam) – 57 counts/sec.; *C* – net fluorescence at zero field – 27 counts/sec.; *D* – field dependent signal (fitted Lorentzian amplitude) – 75 counts/sec.

of reflection of 584 Å radiation from the walls of the Pyrex tubes. Since this effect increases both solid angle corrections by approximately the same factor it can be neglected.

In this background scattering process the incident light direction is parallel to the magnetic field and perpendicular to the observation direction, a 0°-90°-90° geometry. For such a geometry and with unpolarized incident light, there should be no magnetic-field dependence of the scattered intensity. However, the small Lorentzian-like field dependence superimposed on the background count rate of Fig. 6 would be expected if the incident 584 Å radiation were partially polarized. The polarization was determined by measuring the scattering rate for the 584 Å radiation at various positions in a plane perpendicular to the light direction at zero magnetic field. These measurements indicate ≈ 25% polarization in a direction parallel to the velocity of the exciting electrons in the electron gun. This direction is also parallel to the observation direction for the data of Fig. 6. For this polarization and geometry the amplitude of the field dependent signal should be one-third the amplitude of the zero-field count rate. Thus the amplitude of the background field dependent signal should be ≈ 19 counts/sec. This compares satisfactorily with the observed value of ≈ 10 counts/sec.

The shape of the background field dependent signal is badly distorted. This distortion could not be removed by adjusting the geometry. It is possibly due to the fact that along with the 584 Å radiation entering the scattering region there are also charged particles. The presence of these is inferred from the effect of electric fields on the background counting rates. The magnetic field also affects the motion of these charged particles, and this effect can not be separated from the magnetic field dependence of the 584 Å scattering rate. In any case, the effects of the background are eliminated in the present experiment by subtracting the background count rate (lamp off) at each magnetic field point from the 2-μ induced count rate (lamp on). This gives the net 584 Å fluorescence.

An estimate of the net fluorescence at zero field (lamp on) can be made by assuming negligible detector solid angle, ( $\beta = \delta = 0^\circ$ ), and uniform intensity from the light pipe over the solid angle determined by  $\Theta_m$ , ( $\alpha = 33^\circ$ ). With these angles and the field dependent amplitude from Fig. 6 in conjunction with Eq. (4), a value of 20 counts/sec is calculated for the net fluorescence at zero field. Considering the uncertainties in the solid angle estimates, this is good agreement with the observed value of 27 counts/sec.

### C. Data Analysis

Half-widths were determined from the data by

means of a least-squares fit to an equation of the form

$$R(H) = A \left( 1 - \frac{1 - Bx}{1 + x^2} \right) + C, \quad x = H/H_{1/2}, \quad (7)$$

where the fitting parameters are  $A$ , the inverted Lorentzian amplitude;  $B$ , a measure of the dispersive component in  $R(H)$ ;  $C$  the scattering rate at zero field; and  $H_{1/2}$ , the half-width at half-maximum. The extent to which the solid angles of incident and detected radiation are not symmetric about perpendicular directions is measured by  $B$ . It has its origin in the third term of Eq. (2). Standard deviations on the fitting parameters were calculated by the usual techniques.<sup>22</sup> Figure 7 shows an example of the 584 Å count rate as a function of the magnetic field. The data for negative and positive fields are the scattering rates for opposite directions of the field. These data were normalized by subtracting the fitted parameter  $C$  and dividing by the fitted Lorentzian amplitude  $A$ .

The line shape is in good agreement with theory up to  $H = \pm 2H_{1/2}$ . However, at larger fields the experimental points always lie below the fitted curve.<sup>23</sup> Anderson<sup>13</sup> observed a similar effect in xenon and suggested that the deviation may be due to an effective decrease in the intensity of the incident light at the larger magnetic fields. This could occur because the frequencies for resonant absorption shift with field and move onto the shoulder of the Doppler broadened line from the lamp. The present experiment is particularly sensitive to such an effect. With a value of  $5.6 \times 10^{-10}$  sec for the lifetime of the  $2^1P$  state, the natural absorption breadth for 2-μ light is

$$\Delta\lambda_N = \lambda^2 / 2\pi c \tau = 0.037 \text{ Å}.$$

The atom temperature in the lamp is taken as ≈ 800°K. In this case the fractional intensity at two natural linewidths,  $2\Delta\lambda_N$ , from the central

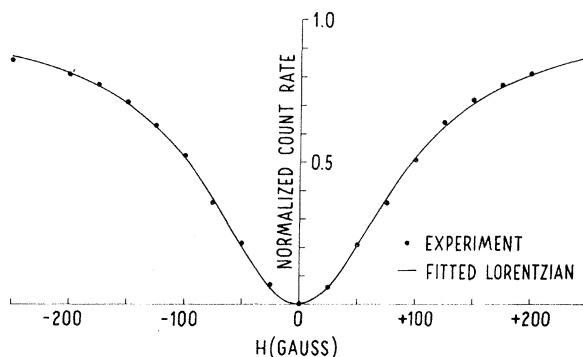


FIG. 7. Normalized 584 Å counting rate versus magnetic field for both directions of field (+ and -).

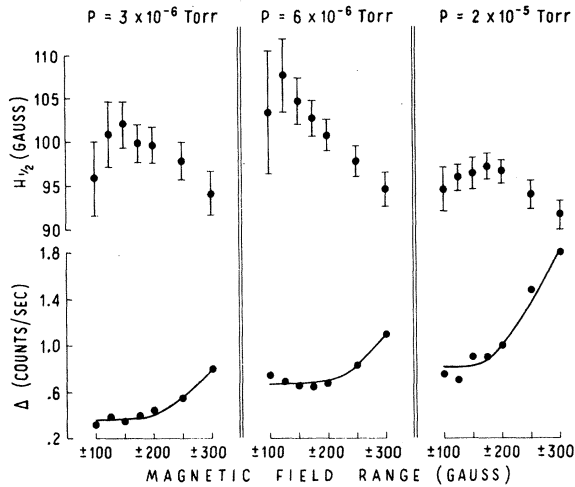


FIG. 8. Results of the least-squares fits as a function of the range of magnetic field.

wavelength is  $0.71$ . Hence, the incident  $2\text{-}\mu$  intensity would be down by 29% at two natural linewidths from the center, and deviations in the inverted Lorentzian at  $H = \pm 2H_{1/2}$  would be expected. However, since the deviations at  $|H| = 2H_{1/2}$  are so small, the effective width of the lamp line is apparently further increased by mechanisms such as pressure broadening, current broadening, or a slight self-reversal. This is consistent with the broadening of the helium lamp profile observed by Burger and Lurio.<sup>24</sup> Actually a weak self-reversal in the  $2\text{-}\mu$  line would be advantageous here, since this would increase the range of wavelengths over which the  $2\text{-}\mu$  line is approximately flat.

Since the data deviate from a Lorentzian at the larger magnetic fields, it is necessary to investigate the quality of the least-squares fit as a function of the range of magnetic field. The results for three different helium background pressures is summarized in Fig. 8. The abscissa give the range of magnetic field for which data is included in the fit. Plotted are  $H_{1/2}$  in gauss, with error bars corresponding to one standard deviation, and  $\Delta$ , the rms deviation per data point. When the larger ranges of field are used the error in  $H_{1/2}$  increases due to the deviations at high field. The rapid increase in  $\Delta$  is the most evident effect produced by these deviations from the Lorentzian line

TABLE 1. Dependence of the linewidth on background pressure.

$P_{\text{He}}$ ( $10^{-6}$ Torr)	$H_{1/2}$ (G)	$A_2\gamma$
3	$99.7 \pm 2.1$	0.01
6	$100.8 \pm 1.8$	0.02
20	$96.9 \pm 1.5$	0.07

shape. The decrease in the fitted  $H_{1/2}$  at large ranges of field occurs consistently since the best fitted amplitude  $A$  must decrease when the high-field data points are included. If  $A$  decreases, then the magnetic field for which the Lorentzian amplitude is  $\frac{1}{2}A$  is also smaller. The range of magnetic field used to determine  $H_{1/2}$  at each pressure is that range which gives smallest error bars on  $H_{1/2}$ . This is also approximately the largest range of field it is possible to use before  $\Delta$  begins to increase rapidly. The best values for  $H_{1/2}$  together with the corresponding pressures in the scattering region are given in Table I. The errors are one standard deviation.

Both the electron gun and the Channeltron detector were shielded with mu metal. The Helmholtz field was then found to have no observable effect on the Channeltron counting rates and produced less than 1% effect on the magnetic field in the electron gun. The effect of the Helmholtz field on lamp intensity was also  $< 1\%$ .

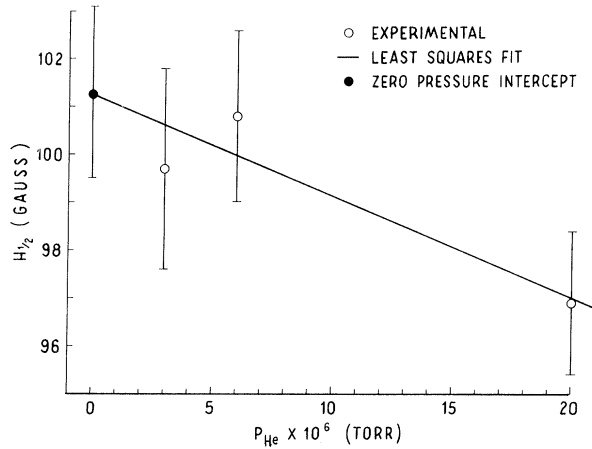
Changing the lamp intensity by 50% had no perceptible effect on line width. Finally, the least-squares parameter  $B$  was always  $< 0.005$ , hence the asymmetry in the line shape was less than 0.5%.

If the density of ground-state helium atoms in the scattering region is sufficiently high, it is possible for the  $584 \text{ \AA}$  radiation to be scattered several times before reaching the detector. Multiple scattering of the  $584 \text{ \AA}$  radiation in the magnetic field region leads to a narrowing of the width of the Lorentzian line shape. This effect has been investigated theoretically<sup>25</sup> and experimentally.<sup>13, 26</sup> Using Eq. (6) with the result of D'yakonov and Perel',<sup>25</sup> the relation between the observed half-width,  $H_{1/2}$ , and the natural half-width,  $H_{1/2}^0$ , is

$$H_{1/2}/H_{1/2}^0 = 1 - A_2\gamma.$$

$A_2$  is a fraction less than one determined by the total angular momenta of the atomic states involved in the scattering.  $\gamma$  is the absorption<sup>21</sup> which is a function of the characteristic dimension  $L$  of the scattering region and of the density of scatterers. For the present experiment  $A_2 = 0.7$  and  $L \approx 1$  cm. The quantity  $A_2\gamma$  is the fractional narrowing. The calculated value of this quantity at each helium pressure is given in Table I.

In the present experiment the absorption is small,  $\gamma \ll 1$ . In this case  $\gamma$  is proportional to the number density of scattering atoms and therefore  $H_{1/2}$  is linearly related to pressure.  $H_{1/2}$  versus pressure is plotted in Fig. 9. The least-squares fit of a straight line to these data results in a zero-pressure intercept (natural half-width)  $H_{1/2}^0 = (101.3 \pm 1.8)\text{G}$ . In order to include the systematic error due to high-field deviations from inverted Lorentzian line shapes, the above error

FIG. 9. The dependence of  $H_{1/2}$  on pressure.

was doubled, with the result

$$H_{1/2}^0 = (101 \pm 4) \text{ G.}$$

The corresponding result for the mean lifetime calculated from Eq. (6) is

$$\tau(2^1P) = (5.63 \pm 0.22) \times 10^{-10} \text{ sec,}$$

where it is assumed  $g_J = 1.0$ .

## V. DISCUSSION

The total transition rate for an electric-dipole transition from a state  $n$  to a state  $n'$  of lower energy is given by<sup>27</sup>

$$A_{n',n} = (32\pi^3 e^2 / 3\hbar \lambda_{n',n}^3) |\vec{r}_{n',n}|^2, \quad (8)$$

where  $\lambda_{n',n}$  and  $|\vec{r}_{n',n}|$  are, respectively, the wavelength and dipole matrix element for the transition. This can be rewritten

$$A_{n',n} = \frac{8\pi^2 e^2}{mc} \frac{g_{n'}}{g_n} \frac{f_{n,n'}}{\lambda_{n',n}^2}, \quad (9)$$

where  $g_{n'}$  and  $g_n$  are the statistical weights of the respective states and  $f_{n,n'}$  is the absorption oscillator strength for the transition  $n'$  to  $n$ . The reciprocal of the mean lifetime of the state  $n$  is given by

$$\frac{1}{\tau_n} = \sum_{E_{n'} < E_n} A_{n',n}, \quad (10)$$

where  $E_n$  is the energy of the  $n$ th state.

If  $f_{2^1P, 2^1S} \approx f_{2^1P, 1^1S}$  (the theoretical values quoted by Schiff and Pekeris<sup>3</sup> are 0.376 and 0.276,

respectively), then it can be shown from Eq. (9) that

$$A_{2^1S, 2^1P} / A_{1^1S, 2^1P} \approx 10^{-3}.$$

Therefore the contribution to  $\tau(2^1P)$  from the  $2^1P$ - $2^1S$  transition is negligible within the present experimental accuracy. Using Eqs. (9) and (10), the absorption oscillator strength,  $f_{2^1P, 1^1S}$ , can be related to  $\tau(2^1P)$  by

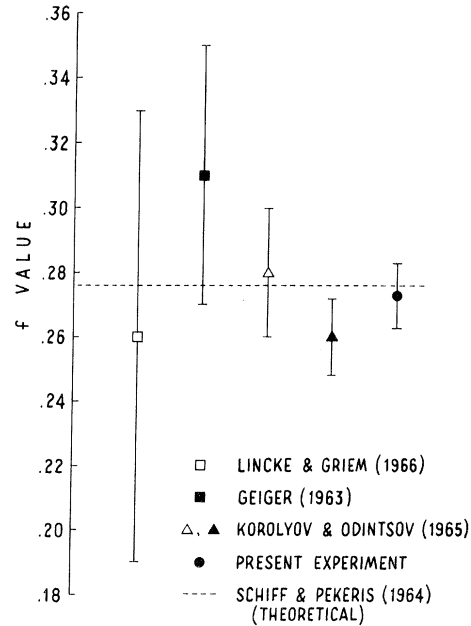
$$f\tau = \frac{mc}{8\pi^2 e^2} \frac{g_{2^1P}}{g_{1^1S}} \lambda^2 = 1.53 \times 10^{-10} \text{ sec.} \quad (11)$$

The resulting oscillator strength for the  $1^1S$ - $2^1P$  transition with the present value of  $\tau(2^1P)$  is

$$f = 0.273 \pm 0.011.$$

This agrees well with the theoretical result obtained by Schiff and Pekeris,<sup>3</sup>  $f = 0.276$ . Figure 10 shows the comparison of the present result with this theoretical result and with the following experimental results.

(1) Korolyov and Odintsov<sup>7</sup> performed interferometric profile analyses of helium lines terminating in the  $2^1P$  state. These lines were ob-

FIG. 10.  $f$  values for the  $1^1S$ - $2^1P$  transition in  $^4\text{He}$ .



tained from a light source produced by electron bombardment of an atomic beam. They had considerable Doppler widths owing to the inelastic collisions with the exciting electrons. For the  $6678 \text{ \AA}$  ( $3^1D-2^1P$ ) line where the conditions for determining the natural width were most favorable, they found  $f = 0.26 \pm 0.012$ . However, the results from other lines studied gave the average value,  $f = 0.28 \pm 0.02$ .

(2) Lincke and Griem<sup>28</sup> studied the Stark broadened emission profile of the resonance line itself and found  $f = 0.26 \pm 0.07$ .

(3) Geiger<sup>29</sup> measured the scattering cross section of 25-keV electrons from helium and obtained  $f = 0.31 \pm 0.04$ .

The present experiment yields a more precise  $f$  value for the  $1^1S-2^1P$  transition in helium than

was previously available. The result agrees with the theoretical  $f$  value for this transition.

This experiment also demonstrates a new technique which can be used to measure the lifetime of certain atomic states. The technique is particularly useful when the strong radiative transitions from these states are in the far ultraviolet.

Finally, it has been shown that the inclusion of solid angle contributions in a level-crossing experiment can reduce the ratio of field dependent to field independent signal from the optimum ratio.

#### ACKNOWLEDGMENTS

The authors would like to acknowledge useful discussions with Professor D. K. Anderson, Professor R. R. Lewis, Professor R. T. Robiscoe, and James Burger.

\*This work was supported in part by the U. S. Atomic Energy Commission and the University of Michigan Office of Research Administration.

†Based on a thesis submitted by E. S. Fry to the Department of Physics, University of Michigan, in partial fulfillment of the requirements for the Ph. D. degree.

‡Present address: Department of Physics, Texas A & M University, College Station, Texas 77843.

<sup>1</sup>A. Dalgarno and N. Lynn, Proc. Phys. Soc. (London) **A70**, 802 (1957).

<sup>2</sup>C. L. Pekeris, Phys. Rev. **112**, 1649 (1958); **126**, 1470 (1962); **127**, 509 (1962); C. L. Pekeris, B. Schiff and H. Lifson, *ibid.* **126**, 1057 (1962).

<sup>3</sup>B. Schiff and C. L. Pekeris, Phys. Rev. **134**, A638 (1964).

<sup>4</sup>A. Dalgarno and A. L. Stewart, Proc. Phys. Soc. (London) **A76**, 49 (1960); E. E. Salpeter and M. H. Zaidi, Phys. Rev. **125**, 248 (1962); L. C. Green, N. C. Johnson, and E. K. Kolchin, Astrophys. J. **144**, 369 (1966); A. W. Weiss, J. Res. Natl. Bur. Std. (U.S.) **71A**, 163 (1967).

<sup>5</sup>H. G. Kuhn and J. M. Vaughan, Proc. Roy. Soc. (London) **A 277**, 297 (1964).

<sup>6</sup>J. M. Vaughan, Phys. Letters **21**, 153 (1966); Proc. Roy. Soc. (London) **A295**, 164 (1966).

<sup>7</sup>F. A. Korolyov and V. I. Odintsov, Opt. i Spektroskopiya **18**, 968 (1965) [English transl.: Opt. Spectry. **18**, 547 (1965)].

<sup>8</sup>A. C. G. Mitchell and M. W. Zemansky, Resonance Radiation and Excited Atoms (Cambridge University Press, New York, 1934), Chap. V.

<sup>9</sup>A. Lurio, R. L. deZafra, and R. J. Goshen, Phys. Rev. **134**, A1198 (1964).

<sup>10</sup>W. L. Williams and E. S. Fry, Phys. Rev. Letters **20**, 1335 (1968).

<sup>11</sup>G. Breit, Rev. Mod. Phys. **5**, 91 (1933).

<sup>12</sup>P. A. Franken, Phys. Rev. **121**, 508 (1961); M. E. Rose and R. L. Carovillano, *ibid.* **122**, 1185 (1961); H. H. Stroke, G. Fulop, S. Kelpner, and O. Redi, Phys. Rev. Letters **21**, 61 (1968).

<sup>13</sup>D. K. Anderson, Phys. Rev. **137**, A21 (1965).

<sup>14</sup>F. D. Colegrove, P. A. Franken, R. R. Lewis, and R. H. Sands, Phys. Rev. Letters **3**, 420 (1959).

<sup>15</sup>M. C. Johnson, Rev. Sci. Instr. **40**, 311 (1969).

<sup>16</sup>F. C. Fehsenfeld, K. M. Evenson, and H. P. Broida, Rev. Sci. Instr. **36**, 294 (1965).

<sup>17</sup>Handbook of Military Infrared Technology, edited by W. Wolfe (U. S. Office of Naval Research, Department of the Navy, Washington, D. C., 1965), p. 430.

<sup>18</sup>M. Fred, F. S. Tomkins, J. K. Brody, and M. Hamermesh, Phys. Rev. **82**, 406 (1951).

<sup>19</sup>J. B. French and J. W. Locke, in Rarefied Gas Dynamics, edited by C. L. Brundin (Academic Press, Inc., New York, 1967), p. 1461.

<sup>20</sup>E. S. Fry and W. L. Williams, Rev. Sci. Instr. (to be published).

<sup>21</sup>Absorption is used as defined by A. C. G. Mitchell and M. W. Zemansky, Ref. 8. The absorption and emission lines were assumed to have pure Doppler widths corresponding to  $T = 300^\circ \text{K}$ .

<sup>22</sup>Y. Beers, Introduction to the Theory of Error (Addison-Wesley Publishing Co., Inc., Reading, Mass., 1962).

<sup>23</sup>This has also been observed by Burger and Lurio who are performing a measurement similar to the one reported here (private communication).

<sup>24</sup>J. Burger and A. Lurio, Phys. Rev. Letters **22**, 755 (1969).

<sup>25</sup>J. P. Barrat, J. Phys. Radium **20**, 541, 633, 657 (1959); M. I. D'Yakonov and V. I. Perel', Zh. Eksperim. i Teor. Fiz. **47**, 1483 (1964) [English transl.: Soviet

Phys. — JETP 20, 997 (1965)].

<sup>26</sup>A. Lurio and R. Novick, Phys. Rev. 134, A608 (1964).

<sup>27</sup>H. A. Bethe and E. E. Salpeter, Quantum Mechanics

of One- and Two-Electron Atoms (Springer-Verlag, Berlin, 1957).

<sup>28</sup>R. Lincke and H. R. Griem, Phys. Rev. 143, 66 (1966).

<sup>29</sup>J. Geiger, Z. Physik 175, 530 (1963).

PHYSICAL REVIEW

VOLUME 183, NUMBER 1

5 JULY 1969

## Calculation of Bremsstrahlung Cross Sections with Sommerfeld-Maue Eigenfunctions

Gerhard Elwert and Eberhard Haug

*Lehrstuhl für Theoretische Astrophysik der Universität Tübingen, Tübingen, Germany*

(Received 11 December 1967; revised manuscript received 16 August 1968)

A formula for the differential cross section of bremsstrahlung is calculated with the aid of Sommerfeld-Maue eigenfunctions, i.e., under the assumption of a pure Coulomb field and low atomic numbers ( $\alpha Z \ll 1$ ). This expression is valid for all energies of both electrons and photons, and it is shown that the previously well-known formulas of Sommerfeld, Sauter, Bethe, Heitler, Scherzer, and Bethe and Maximon are contained as special cases. Hence this cross section is correct for high electron energies and, apart from a small spin correction, for nonrelativistic energies even if  $\alpha Z \ll 1$  is not satisfied. The formula has been programmed, and in addition total cross sections have been obtained by numerical integration over the angles of the emitted electrons and photons. Comparison with the Born approximation allows derivation of the Coulomb correction. Several cases of interest are compared with experiment, in particular the elementary bremsstrahlung process itself, for which experimental results are now available.

### 1. INTRODUCTION

The theory of bremsstrahlung has been the subject of a large number of papers in which various energy regions and different types of approximation for the interaction of the electrons with the atomic field have been considered. Whereas presently at any rate the interaction of electrons with the radiation field can be treated only by perturbation theory, their interaction with the field of the atomic nucleus can in principle be handled rigorously. In the latter case one uses as eigenfunctions for the electrons the exact Coulomb solutions for the nuclear electrostatic field, such that these solutions correspond asymptotically to plane waves and incoming or outgoing spherical waves.

Actually this treatment amounts to summing over-all (infinitely many) Feynman graphs representing the interaction of electrons with the nuclear field. In this way Sommerfeld<sup>1</sup> was the first to calculate the matrix element with Schrödinger eigenfunctions for the nonrelativistic case. For the relativistic energy domain it is also possible to use the same method at least in principle, but so far exact solutions for the Dirac equation including the Coulomb field with the above bound-

ary conditions have only been found in series form as a summation over quantum number  $l$ .<sup>2</sup> Because of the large number of summands appearing in the matrix element, it would be extremely troublesome to perform these calculations numerically.

In fact, Sommerfeld and Maue<sup>3</sup> have already given a relativistic eigenfunction which is correct up to first order in  $\alpha Z$ . Using the Sommerfeld-Maue eigenfunction, Elwert<sup>4</sup> first calculated the matrix element of the elementary process of the x-ray emission. His result was only reported<sup>4</sup> but not published in detail as the evaluation of the expression obtained was then (1938) too complicated to be performed. In the present paper we further develop the above expression for the differential cross section and apply it for various cases of interest. We obtain the formulas of Sommerfeld,<sup>1</sup> Sauter,<sup>5</sup> Bethe and Heitler,<sup>6</sup> and Scherzer<sup>7</sup> as special cases.

The theoretical differential cross section is compared with new coincidence experiments. The differential cross section has also been integrated numerically over the direction of the outgoing electrons and photons to obtain several comparisons between theory and experiment.